Journal of Catalysis **189,** 410–420 (2000)
doi:10.1006/jcat.1999.2708, available online at http://www.idealibrary.com on IDEAL®

Role of the Nature of the Support (Alumina or Silica), of the Support Porosity, and of the Pt Dispersion in the Selective Reduction of NO by C_3H_6 under Lean-Burn Conditions

Patricia Denton, Anne Giroir-Fendler, Hélène Praliaud,[1] and Michel Primet

Laboratoire d'Application de la Chimie à l'Environnement (LACE), UMR 5634 (CNRS-UCB Lyon 1), 43, boulevard du 11 novembre 1918, 69622 Villeurbanne Cedex, France

Received June 17, 1999; revised August 27, 1999; accepted September 28, 1999

During selective reduction of NO_x under lean-burn conditions, a Pt particle size dependency has previously been observed with various supports. In this study, we have examined the influence of various parameters over a large range of initial metal dispersion: nature of the support (silica or alumina), support porosity, presence of impurities (particularly chlorine or sulfur), nature of the platinum precursor salt, and Pt particle size distribution. Furthermore, we have considered the mean particle size after sintering under the reactant mixture up to 773 K. Of the factors considered, only the Pt dispersion is of key importance. The intrinsic activity increases with decreasing dispersion (measured initially or after reaction) for each of the main reactions: reduction of NO into N_2 or N_2O, oxidation of NO into NO_2, or oxidation of C_3H_6 into CO_2. The dispersion does not clearly affect the selectivity. © 2000 Academic Press

Key Words: **DeNO$_x$; selective nitric oxide reduction; SCR NO; Pt-supported catalysts; dispersion; support effects.**

INTRODUCTION

Supported noble metal catalysts, particularly those containing platinum, are active for the selective reduction of NO by hydrocarbons at relatively low temperatures (1–5) and are not significantly affected by the presence of water (4,6,7). The maximum activity of noble metal catalysts occurs at a lower temperature (473–623 K) than that of Cu–zeolite catalysts (573–723 K) (8). Contrary to Cu–zeolites, however, these solids present a narrow activity–temperature window (1–5) and form substantial amounts of N_2O (2,4,5,9). It has been reported that the activity depends on the choice of SiO_2 or Al_2O_3 as support (9–11) and on the Pt dispersion (2,5,12). Other results, however, bring into question the effect of the nature of the support (13,14) and the metal dispersion (15,16) on activity and/or selectivity. Furthermore, the particle size dependency can be affected not only by the nature of the support (17) but also by the reaction considered: NO dissociation, NO reduction, NO oxidation, or C_3H_6 oxidation (17–20).

With Cu–zeolite catalysts the activity depends on the nature of the zeolite (21); possible factors include proton acidity and the size of cavities or channels, since small-channeled zeolites provide the benefit of enhanced N–N pairing (22). In this study, we have investigated the effect of the support porosity of conventional Pt-based alumina and silica catalysts, as well as the influence of Pt dispersion, measured initially and after contact with the reactant mixture. Other parameters considered are support impurities, preparation procedure, Pt precursor salt, and Pt particle size distribution (homogeneous or not).

METHODS

2.1. Apparatus

In general, a laboratory-made apparatus was used to determine the N_2 adsorption isotherm at 77 K. The specific surface area, the pore size distribution, and the porous volume were deduced from this isotherm. For the microporous supports, however, low-pressure data were obtained with a Micromeritics ASAP 2000 apparatus. Prior to the measurements, the samples were evacuated at 773 K for 2 h, except for the microporous silica supports (423 or 573 K). The specific surface area was determined from the linear portion of the BET plot using the data below $P/P_o = 0.3$. The cumulative pore surface, the pore size distribution, and the average pore radius ($2V/S$) were calculated from the desorption branch of the N_2 isotherm using the BJH method or Roberts's method. The microporous volume and microporous surface were deduced from the *t*-plot of DeBoer (23). The MP method (model-less pore method), which applies to pores of any shape and leads to a hydraulic pore radius (V/S), was also used with the microporous solids (24).

Adsorption measurements were conducted in a conventional volumetric apparatus. The catalysts were reduced

[1] To whom correspondence should be addressed. Fax: (33) 4 72 44 81 14. E-mail: praliaud@univ-lyon1.fr.

0021-9517/00 $35.00

overnight *in situ* at 573 K under H_2, cooled to room temperature under H_2, and then evacuated at 573 K for 2 h. The irreversible chemisorption uptake of H_2 was measured at 298 K. The accessible metallic surface was calculated assuming that one Pt atom occupies 1×10^{-19} m^2 with a 1 H, 1 Pt stoichiometry. For TEM analysis, a sample of reduced catalyst was reexposed to air and suspended in ethanol, a drop of this suspension was deposited on a carbon-coated grid, and the specimen was examined with a high-resolution JEOL 2010 electron microscope.

The SCR activity measurement was conducted in a fixed-bed quartz reactor in a flow system at atmospheric pressure, as already described (25–27). A 0.2-g sample of reduced catalyst, with grain diameters between 50 and 100 μm, was used. The typical reactant gas composition was 2000 vpm NO, 2000 vpm C_3H_6, 5 vol% O_2, and He as carrier gas (total flow rate 10 L h^{-1}). Each experiment was conducted as follows:

—*in situ* re-reduction by H_2 at 573 K,
—introduction of the mixture at 423 K,
—heating from 423 to 773 K at a rate of 1.8 K min^{-1},
—plateau at 773 K for 1 h,
—cooling from 773 to 298 K.

As already described (25–27), reactants and products (CO_2, N_2O, O_2, N_2, CO, and H_2O) were analyzed by gas chromatography, with He as the carrier gas, using a dual CTR1 column from Alltech (Porapak and molecular sieve) and a TCD detector. A Porapak column and a flame ionization detector were employed for C_3H_6. The mixture was analyzed every 10 or 15 min. In addition, the concentrations of NO, NO_2, N_2O, and CO_2 were continuously measured online by Rosemount IR and UV analyzers. A substantial amount of NO_2 was formed in the pipes of the apparatus, before the reactor and in the exit lines from the reactor, as previously observed (27,28). The 165 vpm NO_2 formed in the pipes was subtracted from total NO_2 before the conversion of NO into NO_2 was calculated. The conversion of NO into N_2 and that of NO into N_2O were also calculated, as was the nitrogen balance including NO_2 formed in the pipes.

The intrinsic activity of reactions [1]–[4] is defined as the number of millimoles of NO or C_3H_6 converted into N_2, N_2O, NO_2, or CO_2 per hour and per m^2 of Pt initially present or per m^2 of Pt present after a standard experiment with the reactant mixture (mmol NO or C_3H_6 h^{-1} m^{-2} Pt). Each intrinsic activity was calculated for particular conditions, namely:

—at a given temperature at which the conversion is below the maximum, with the conversion varying among catalysts;
—at a given conversion, with the temperature varying among catalysts;
—at the maximum of conversion, with the conversion and the temperature varying among catalysts.

The intrinsic activity of the first three reactions was directly calculated from the concentration of N_2, N_2O, and NO_2. That of the fourth reaction was obtained by subtracting the CO_2 formed by reactions [1] and [2] from total CO_2.

$$NO + 1/9\,C_3H_6 \rightarrow 1/2\,N_2 + 1/3\,CO_2 + 1/3\,H_2O \quad [1]$$

$$NO + 1/18\,C_3H_6 \rightarrow 1/2\,N_2O + 1/6\,CO_2 + 1/6\,H_2O \quad [2]$$

$$NO + 1/2\,O_2 \rightarrow NO_2 \quad [3]$$

$$C_3H_6 + 9/2\,O_2 \rightarrow 3\,CO_2 + 3\,H_2O \quad [4]$$

2.2. The Supports

The nonporous alumina and silica supports (type II nitrogen isotherm) were provided by Degussa and were prepared by flame hydrolysis of $AlCl_3$ and $SiCl_4$. The mesoporous alumina (type IV isotherm), from Rhodia, was prepared by precipitation from an aluminum sulfate solution by NaOH. The mesoporous silica supports, supplied by Grace Davison, were prepared by precipitation from an aqueous silicate solution by diluted H_2SO_4. Both microporous silica supports (type I isotherm) were laboratory-made by sol–gel methods. One (SiO_2 J, Laboratoire des Matériaux et des Procédés Membranaires) was prepared by hydrolysis of tetraethylorthosilicate (TEOS) in acidic medium, followed by addition of a nonionic surface active agent (alkylphenyl polyether alcohol), followed by treatment under air at 723 K (24). The other (SiO_2 P, Institut de Recherches sur la Catalyse) was prepared by hydrolysis of TEOS in basic medium at a pH higher than the isoelectric point of silica, followed by treatment under N_2 at 823 K (29).

Table 1 gives the main characteristics of the supports. For the mesoporous silica, the particle size distribution is narrow and the average pore radius ($2V/S$) deduced from Roberts's method is equal to 3 or 6 nm. For the mesoporous

TABLE 1

The Supports

Name	Origin	S_{BET}	S_{CUM}	S_μ	V_μ
		Alumina			
Meso (6 nm)	Rhodia	154	176	3	0.00064
Nonporous	Degussa	108	81	13	0.00061
		Silica			
Meso (3 nm)	Grace	596	753	0	0
Meso (6 nm)	Grace	341	451	25	0.0064
Micro P	IRC	238	17*	235	0.110
Micro J	LMPM	580	120*	575	0.265
Nonporous	Degussa	202	149	32	0.0125

Note. BET specific surface area, S_{BET} (m^2 g^{-1}); cumulative pore surface area, S_{CUM} (m^2 g^{-1}), deduced from the desorption isotherm with the BJH method* or Roberts's method; microporous volume, V_μ (liquid, mL g^{-1}); and microporous surface area, S_μ (m^2 g^{-1}), deduced from the *t*-plot. IRC, Institut de Recherches sur la Catalyse, Villeurbanne, France. LMPM, Laboratoire des Matériaux et des Procédés Membranaires, Montpellier, France. Meso and micro for mesoporous and microporous.

alumina, the particle size distribution is somewhat larger, with an average pore radius of 6 nm. For the microporous silica, SiO_2 J and SiO_2 P, the average radii deduced from the BJH method are, respectively, 1.1 and 1.0 nm. The MP method gives a hydraulic pore radius (V/S) of 0.44 nm for the SiO_2 J support.

Let us note that the preparation method determines whether sulfur or chlorine will reside as an impurity on the support. For instance, the supports from Degussa, prepared by flame hydrolysis, contain chlorine (<4860 ppm for Al_2O_3 and <240 ppm for SiO_2) but no sulfur (<2 ppm). The alumina from Rhodia, prepared by precipitation, contains 117 ppm of S but no Cl. The silicas from GRACE contain Cl and S (both <300 ppm). The microporous silicas are chlorine- and sulfur-free.

2.3. Preparation of the Catalysts

Table 2 gives the name of each fresh catalyst (designated F), the precursor salt employed, and the method of preparation. The major part of the catalysts contained around 1 wt% Pt.

Generally, platinum was deposited by wet impregnation of the support with a chlorine-free precursor, $Pt(NH_3)_4(OH)_2$, in aqueous solution. In order to obtain a higher dispersion, one of the mesoporous silicas was ion-exchanged with $Pt(NH_3)_4(OH)_2$. To obtain larger particles without unduly broadening the particle size distribution, successive impregnations by $Pt(NH_3)_4(OH)_2$, with intermediate calcinations and reductions, were performed on the mesoporous alumina from Rhodia. For comparison, this chlorine-free alumina was also impregnated with $Pt(C_4H_5O_2)_2$ dissolved in toluene, and with H_2PtCl_6 in aqueous solution. After drying at 393 K, the solids were calcined under air (10 L h^{-1}) at 773 K (heating rate 1 K min^{-1}, plateau 8 h), except for the solid prepared with $Pt(C_4H_5O_2)_2$ (0.5 K min^{-1}) and the ion-exchanged solid (573 K, heating rate 0.5 K min^{-1}).

In order to further decrease the Pt dispersion, the calcined solid prepared by successive impregnations of the mesoporous alumina was reduced under H_2 at 773 K for 2 h and evacuated at 1173 K for 2 h. Another treatment (24 h at 923 K under 10 vol% O_2–10 vol% H_2O–N_2) was used to decrease the dispersion of one of the solids prepared with H_2PtCl_6.

All catalysts were reduced overnight in a flow of hydrogen (3.6 L h^{-1}) at 573 K (2 or 1 K min^{-1}).

RESULTS AND DISCUSSION

3.1. Dispersion and Particle Size of the Fresh Catalysts: Activity Measurements

3.1.1. Dispersion and particle size. The main characteristics of the fresh (F) Pt-supported catalysts are summarized in Table 2. For a given preparation procedure, the dispersion depends on the support: it is high for the microporous silica, moderate for the nonporous supports, and higher for the mesoporous alumina than for the mesoporous silica. The reasons for these support effects are not yet known.

Some of the catalysts have been examined by transmission electron microscopy (Table 2). For the 1F solid prepared by impregnation of the mesoporous alumina with $Pt(NH_3)_4(OH)_2$, we observe heterogeneously dispersed Pt particles between 4 and 15 nm in diameter. This catalyst must also possess smaller particles, since the metallic

TABLE 2

Main Physico-chemical Characteristics of the Catalysts before Reaction (Fresh Catalysts)

Name	Precursor	Pt (wt. %)	Disp. (%)	S (m^2/g Pt)	D_{TEM} (nm)
1F) Pt/meso Al_2O_3 (6 nm)	[a]	1.00	77	191	4–15
2F) Pt/meso Al_2O_3 (SI)	$Pt(NH_3)_4(OH)_2$	1.05	55	135	2
3F) Pt/meso Al_2O_3 (SI) aged	$Pt(NH_3)_4(OH)_2$	1.05	19	46	5
4F) Pt/meso Al_2O_3 (Cl)	H_2PtCl_6	0.96	76	189	
5F) Pt/meso Al_2O_3 (Cl) aged	H_2PtCl_6	2.2	5.2	13	
6F) Pt/Al_2O_3 meso (Acac)	$Pt(C_4H_5O_2)_2$	0.90	94	232	
7F) Pt/nonporous Al_2O_3	[a]	0.77	58	144	
8F) Pt/meso SiO_2 (3 nm)	[a]	0.90	34	83	3
9F) Pt/meso SiO_2 (3 nm) EXC	$Pt(NH_3)_4(OH)_2$	1.05	97	241	undetected
10F) Pt/SiO_2 meso (6 nm)	[a]	0.87	23	56	5
11F) Pt/micro P SiO_2	[a]	0.93	93	229	undetected
12F) Pt/micro J SiO_2	[a]	1.02	100	247	undetected
13F) Pt/nonporous SiO_2	[a]	0.89	47	117	

Note. Weight percent of Pt, metallic dispersion, and metallic surface area determined by H_2 chemisorption, particle diameter deduced from electron microscopy. SI, successive impregnations; SI aged, Pt/meso Al_2O_3 (SI) evacuated at 1173 K after reduction at 773 K; Cl, chlorine-containing precursor; Acac, acetylacetonate-containing precursor; (Cl) aged, treated at 923 K under a 10 vol% O_2–10 vol% H_2O–N_2 mixture; EXC, exchange.

[a] Solid prepared by impregnation of $Pt(NH_3)_4(OH)_2$.

dispersion deduced from H_2 chemisorption (77%) corresponds to a mean particle size of ≈1.5 nm. For the 2F solid prepared by successive impregnations, we observe homogeneously dispersed, spherical Pt particles (Fig. 1) with a 2-nm diameter, in agreement with the dispersion obtained by H_2 chemisorption (55%). After aging under vacuum at 1173 K (solid 3F), the particles are larger (5 nm in diameter), but the particle size distribution remains homogeneous (Fig. 2). For the 8F and 10F solids prepared by impregnation of mesoporous silicas, we observe homogeneously dispersed, 3- (Fig. 3) and 5-nm-diameter Pt particles, in agreement with the sizes deduced from H_2 chemisorption. The preparation by exchange (solid 9F) leads to very small, undetected particles, which is not surprising given the very high dispersion of 97% obtained by H_2 chemisorption. For the solids prepared from the microporous silicas, the particles (diameter around 1 nm) are not detectable, either.

3.1.2. Activity expressed as conversion. Each catalyst is activated under the reaction mixture, regardless of whether it was initially calcined or reduced *in situ*, and regardless of the support, the precursor, and the preparation procedure. Because this activation is more or less pronounced for each catalyst, the values reported here were obtained during the decrease in temperature, once the activity had been stabilized. We note that a pretreatment at 773 K under the mixture stabilizes the catalyst, thereby eliminating the hysteresis in a subsequent temperature increase–decrease cycle. An enhancement of activity during methane combustion has already been observed, particularly for Pt/Al_2O_3 and Pd/Al_2O_3 solids containing chlorine (30–33). In this study, the removal of chlorine-containing species during the reaction is not the main reason for the activation, which is also observed with the chlorine-free Pt/(mesoporous Al_2O_3) solid.

Figure 4 illustrates the overall NO conversion; the conversion of NO into, respectively, N_2, N_2O, and NO_2; and the conversion of C_3H_6 into CO_2, for Pt/mesoporous SiO_2 (3 nm), the most active of the solids containing around 1 wt% Pt. The conversion of NO into N_2 and N_2O reaches 25 and 47%, respectively, at 508 K. The selectivity in N_2O, defined as the ratio $N_2O/(N_2 + N_2O)$, is calculated using the maxima of NO conversion into N_2 and into N_2O and is thus equal to 65%.

The general reaction tendencies are consistent with those already reported in the literature (1,2,34,35). As the temperature rises, the NO conversion increases, passes through a maximum, and then decreases. The reductions of NO into N_2 and N_2O reach maxima at temperatures (488–553 K range) close to that at which the oxidation of propene is nearly complete. It can be noted that Pt is a poor N_2O decomposition catalyst (36,37). Subsequently, at higher temperatures, the NO reduction decreases due to the oxidation of C_3H_6 by O_2, and NO_2 becomes the predominant product. At still higher temperatures, the decrease in NO_2 formation is due to the thermodynamic limitation. Broadly speaking, the stronger the conversion maximum for a given NO-based reaction, the lower the corresponding temperature.

The nitrogen balance (taking into account the NO_2 formed in the pipes) is obtained within 6%. We note that the water formed during the reaction is strongly acidic (pH 1) due to the formation of HNO_2 and/or HNO_3, neither of which is analyzed. Carbon dioxide and water are the only products of propene oxidation; no traces of CO are detected.

3.1.3. Intrinsic activity. The intrinsic activity, namely, the number of millimoles converted per hour and per m^2 of initial accessible metallic surface area, is illustrated as a function of the initial metal dispersion in Figs. 5–9 (fresh catalysts). For the reduction of NO into N_2 (Fig. 5), the maximum intrinsic activity is shown at variable conversion of NO into N_2 and at variable temperature because of the relatively low N_2 concentrations observed. For the three remaining reactions (reduction of NO into N_2O, oxidation of NO into NO_2, oxidation of C_3H_6 by O_2), the intrinsic activities are illustrated either at a given temperature and a variable conversion (Figs. 6 and 7), or at a given conversion and a variable temperature (Figs. 8 and 9).

In general, larger particles lead to higher intrinsic activity for the two supports (alumina–solids 1F to 7F, and silica–solids 8F to 13F). This phenomenon, which seems to be of comparable importance for each reaction, is observed whether the intrinsic activity is calculated at a given, relatively moderate conversion, at a given temperature, or at the maximum of conversion.

For a particular support and precursor (solids 1F, 2F, and 3F; or 4F and 5F; or 8F and 9F) dispersion clearly affects activity. Furthermore, in the following cases, similar dispersion leads to similar activity:

—for a given chlorine-free support and a different precursor (1F and 4F);

—for two Al_2O_3 supports with different porosity and impurities (2F and 7F);

—for three SiO_2 supports with varying porosity (9F, 11F, and 12 F) and one alumina support (6F);

—for one alumina and one silica of the same porosity (3F and 10F).

The other factors (nature and porosity of the support, precursor salt, etc.) are of minor importance. It is noteworthy, however, that the most active solid (5F) happens to be prepared via H_2PtCl_6.

Since this particle size dependency also occurs with homogeneously dispersed particles (solids 2F and 3F, as well as 8F, 9F, 10F, 11F, and 12F), the reactions could be considered as structure-sensitive.

Particle size sensitivity has been reported for propylene oxidation over Pt/Al_2O_3 (38), for methane oxidation over Pt or Pd on alumina (30–33,39), and for NO reduction over

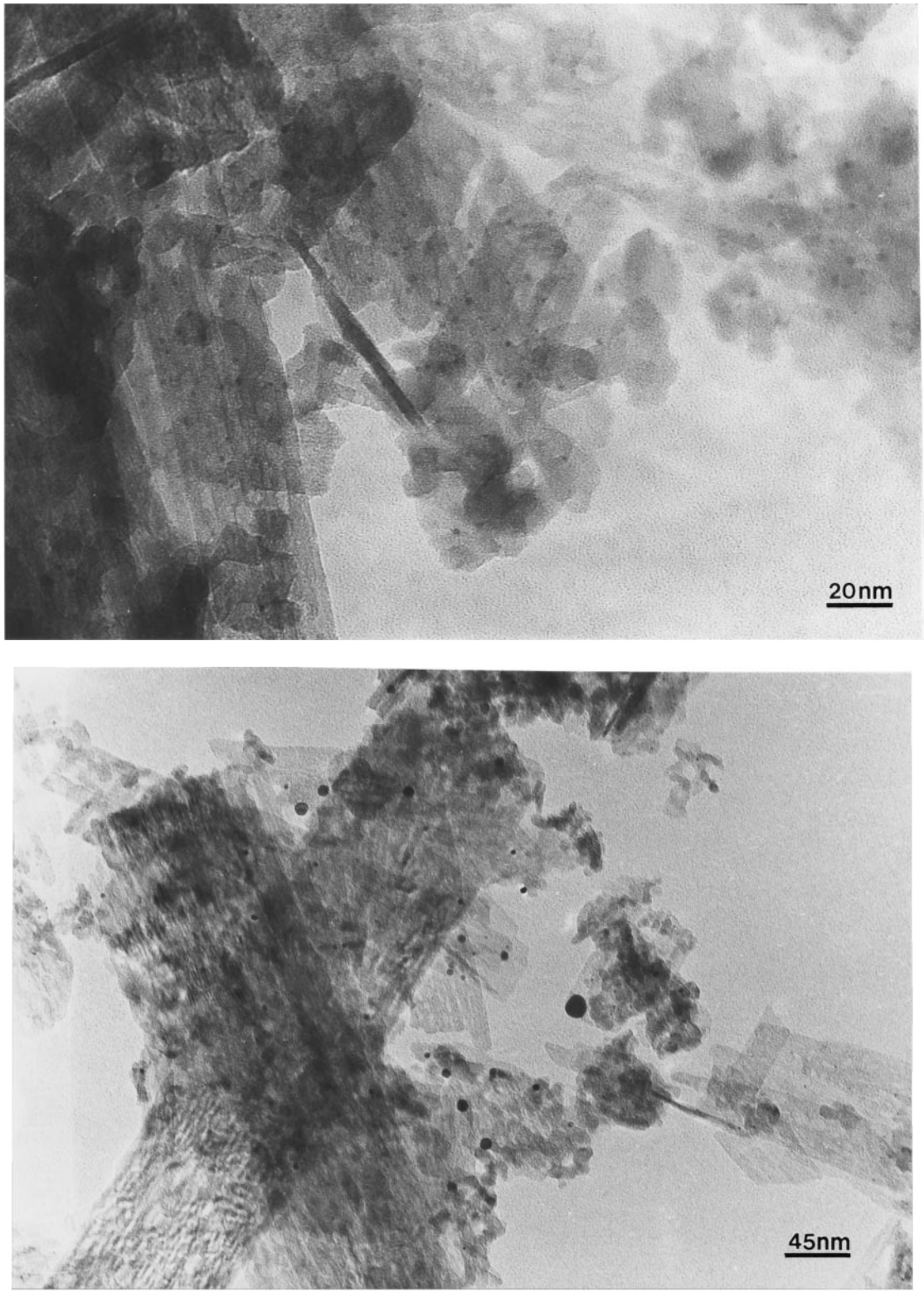

FIG. 1. TEM views of the solid prepared by successive impregnations of the mesoporous alumina, before (solid 2F, top) and after reaction (solid 2U, bottom).

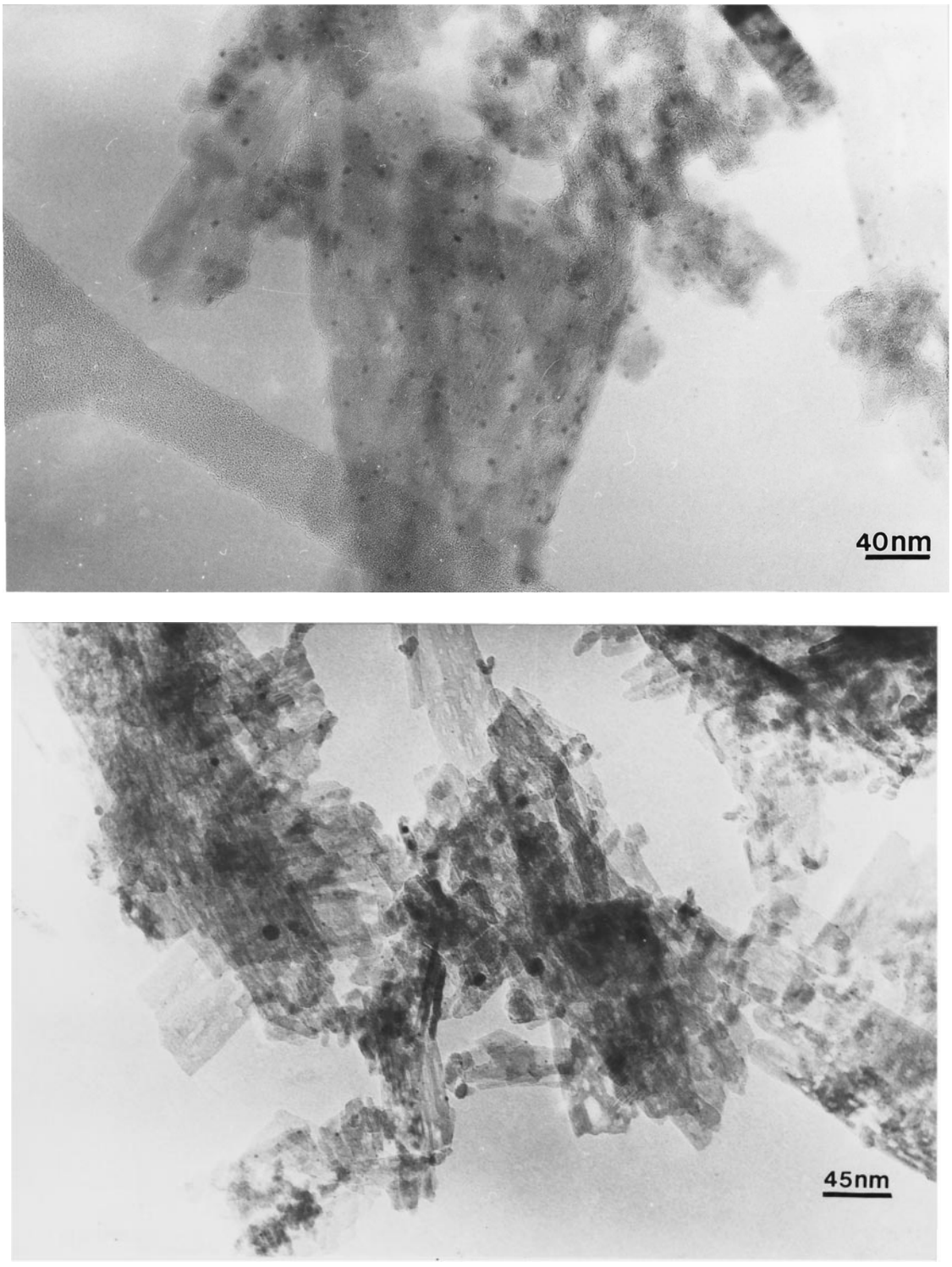

FIG. 2. TEM views of the solid prepared by successive impregnations of the mesoporous alumina and subsequently aged at 1173 K under vacuum, before (solid 3F, top) and after reaction (solid 3U, bottom).

Pd/Al_2O_3 in the presence of near-stoichiometric NO–CO–O_2 mixtures (40).

An intrinsic activity optimum is not obtained even with an initial dispersion as low as 5% (solid 5F), and for a dispersion higher than 40% the intrinsic activity is relatively weak.

Let us emphasize that the initial state of the solid is not representative of the state after activation under the

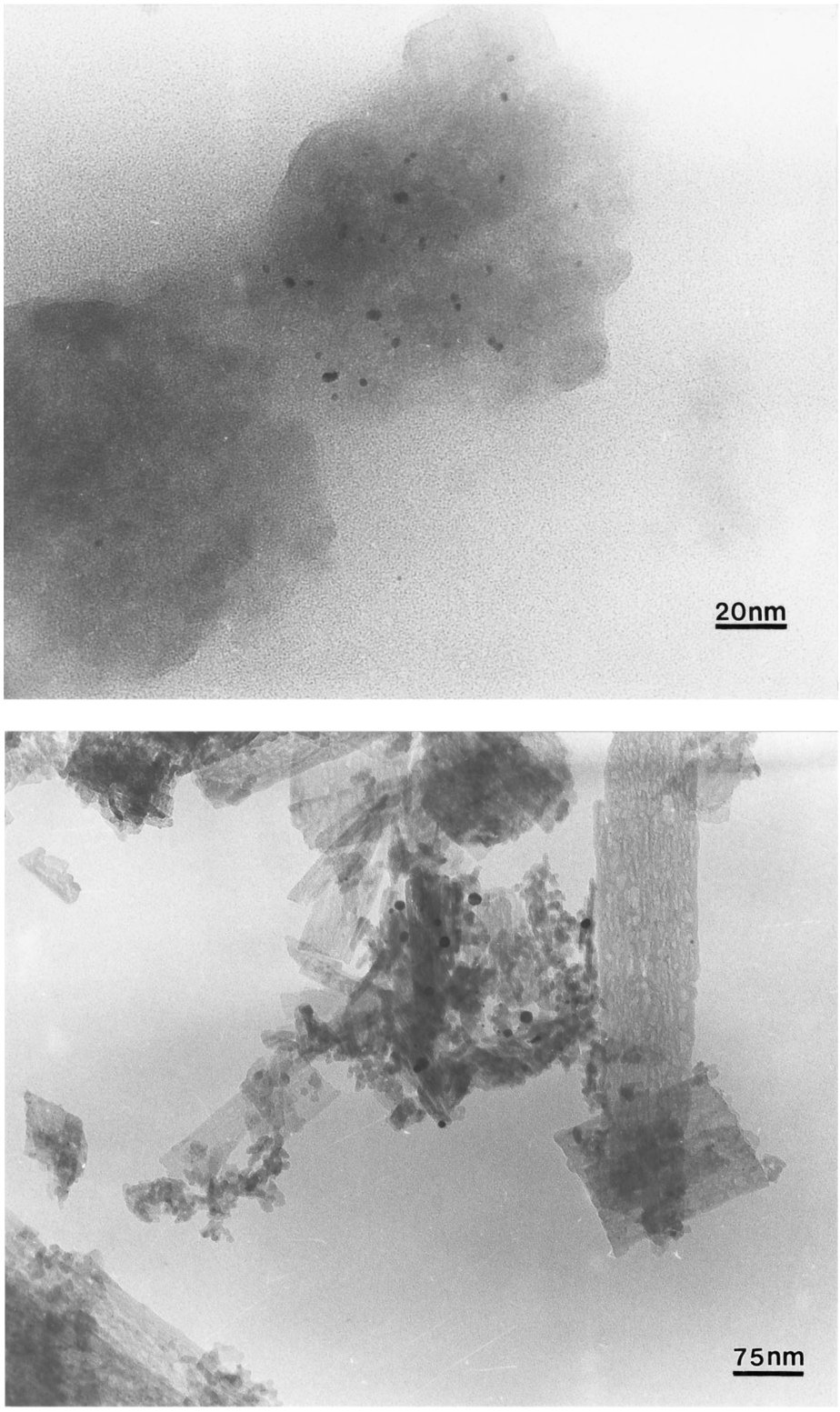

FIG. 3. TEM views of the solid prepared by impregnation of the mesoporous (3 nm) silica, before (solid 8F, top) and after reaction (solid 8U, bottom).

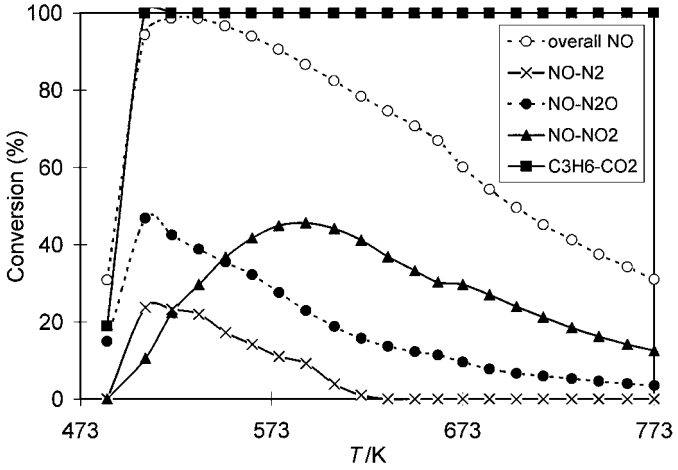

FIG. 4. Overall NO conversion; conversions of NO into N_2, into N_2O, and into NO_2; and overall conversion of C_3H_6 into CO_2, as a function of temperature for Pt/meso SiO_2 (3 nm). The values were obtained during the decrease in temperature. The 165 vpm NO_2 (8% NO into NO_2 conversion) formed in the pipes was subtracted.

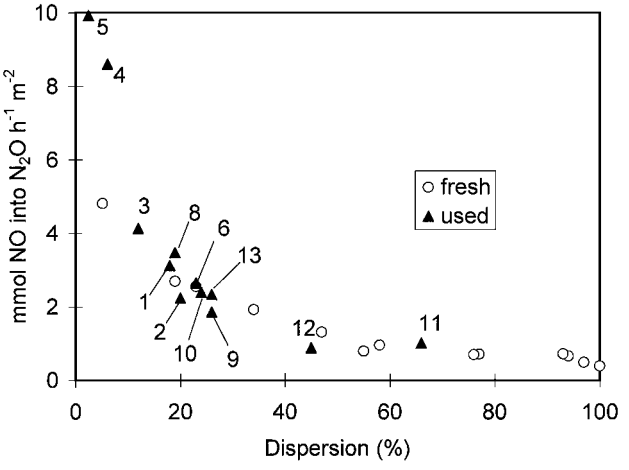

FIG. 6. Number of millimoles of NO converted into N_2O per hour and per m^2 of accessible Pt as a function of Pt dispersion, before and after reaction, at a given temperature, 553 K. Conversion of NO into N_2O between 24% (Pt/micro J SiO_2) and 37% (Pt/micro P SiO_2).

reactants and that the comparison based on the freshly prepared catalysts is of limited value.

3.2. Dispersion and Particle Size after Activation under the Reaction Mixture: Activity Measurements

Particle sintering occurs during activation under the reactants. Accordingly, after reaction and subsequent reduction under H_2 at 573 K, the metallic surface area accessible to H_2 has strongly decreased. The resulting dispersion for these used (U) catalysts is between 12 and 26%, except for Pt on microporous silica supports (dispersions of 66 and 45%) and for Pt/Al_2O_3 solids containing chlorine, either from the support (nonporous alumina) or from the precursor (H_2PtCl_6) (Table 3). The relationship between the initial dispersion and the final dispersion is not clear. We can say that the dispersion decreases more strongly with alumina than with silica and, in the case of alumina, with a chlorine-containing precursor. For instance, the 1F and 4F solids have identical initial dispersion, but, after reaction, the 1U and 4U solids differ in dispersion.

The particle size distribution deduced from transmission electron microscopy has generally widened (Table 3), especially for the solids 2U (Fig. 1), 8U (Fig. 3), and 9U, and to a lesser degree for solid 3U (Fig. 2). Despite the width

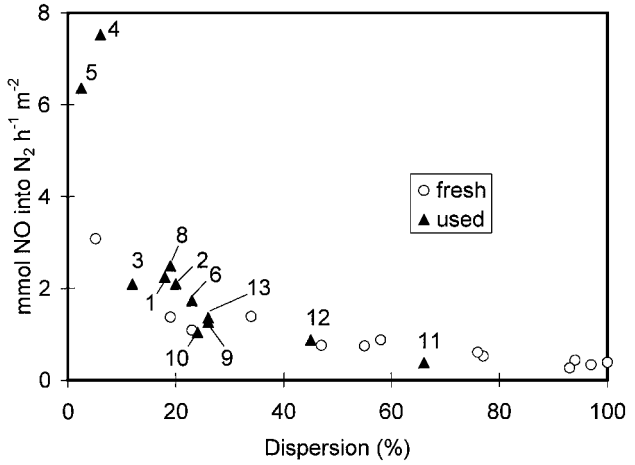

FIG. 5. Maximum number of millimoles of NO converted into N_2 per hour and per m^2 of accessible Pt as a function of Pt dispersion, before and after reaction. Conversion of NO into N_2 between 13% (Pt/meso SiO_2 6 nm and Pt/micro P SiO_2) and 27% (Pt/meso Al_2O_3, Cl). Temperature between 488 K (Pt/meso SiO_2 3 nm EXC) and 543 K (Pt/micro P SiO_2). The used solids are labeled directly on the figure.

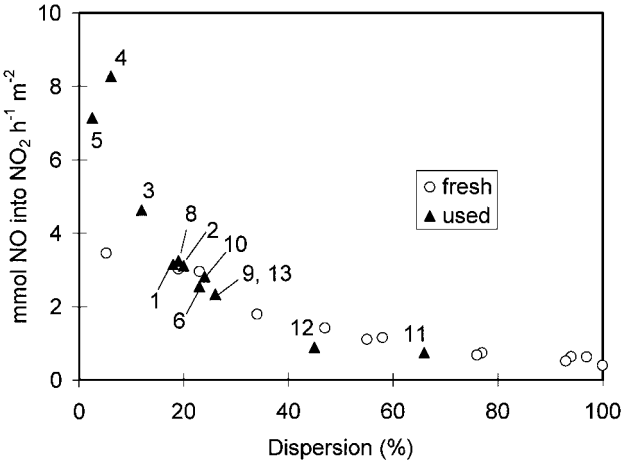

FIG. 7. Number of millimoles of NO converted into NO_2 per hour and per m^2 of accessible Pt as a function of Pt dispersion, before and after reaction, at a given temperature, 673 K. Conversion of NO into NO_2 between 23% (Pt/micro J SiO_2) and 38% (Pt/meso Al_2O_3 SI, and Pt/meso SiO_2 3 nm EXC).

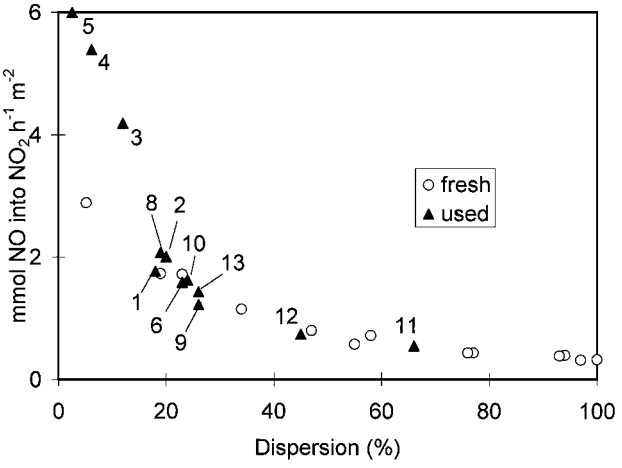

FIG. 8. Number of millimoles of NO converted into NO_2 per hour and per m^2 of accessible Pt as a function of Pt dispersion, before and after reaction, at a given conversion, 20%. Temperature between 498 K (Pt/meso SiO_2 3 nm EXC) and 633 K (Pt/micro J SiO_2).

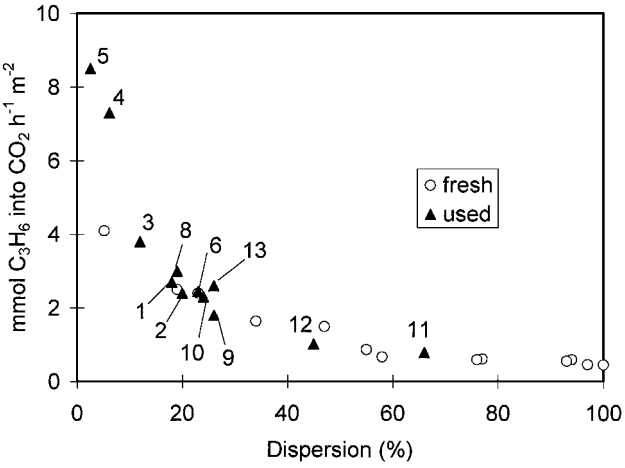

FIG. 9. Number of millimoles of C_3H_6 converted into CO_2 (reaction [4]) per hour and per m^2 of accessible Pt as a function of Pt dispersion, before and after reaction, at a given overall C_3H_6 conversion, 30%. Temperature between 473 K (Pt/meso SiO_2 3 nm EXC) and 513 K (Pt/meso SiO_2 6 nm).

of the particle size distribution, the size deduced from H_2 chemisorption is within the range observed by electron microscopy for the 2U, 3U, and 8U solids, but, according to the average particle size deduced from H_2 chemisorption, solids 1U and 9U also possess smaller particles not detected by TEM. Generally, after reaction, the particle size distribution is large and a mean diameter is not calculable without a prohibiting number of measurements.

For all reactions, the intrinsic activity calculated from the metallic surface area measured after reaction clearly increases with decreasing dispersion (points identified on the figures). This dependency occurs even in a very narrow range of dispersion (18–26%). The activity increases strongly as the dispersion decreases below 18%. No optimum is obtained, even with a dispersion as low as 2.6%, except for maximum NO–N_2 (Fig. 5) and for NO–NO_2 at 673 K (Fig. 7), for which solid 4U is the most active. This, however, is not necessarily representative, since this maximum is not obtained for the NO–NO_2 reaction when the rates are measured at isoconversion (Fig. 8).

The other parameters are minor factors, even in a narrow range of dispersion: we can compare solids 1U and 8U (alumina and silica, both mesoporous, prepared from the same chlorine-free precursor), solids 2U and 6U (same alumina and two chlorine-free precursors), and solids 10U and 13U (silica supports with various porosity and same chlorine-free precursor). The influence of the support and of the

TABLE 3

Main Physico-chemical Characteristics of the Catalysts after Reaction (Used Catalysts)

Name	Disp. (%)	S (m^2/g Pt)	D_{H_2} (nm)	D_{TEM} (nm)
1U) Pt/meso Al_2O_3 (6 nm)	18	44	6.3	8–16
2U) Pt/meso Al_2O_3 (SI)	20	48	5.7	3–15
3U) Pt/meso Al_2O_3 (SI) aged	12	30	9.5	5–10
4U) Pt/meso Al_2O_3 (Cl)	6, 2	15	18	
5U) Pt/meso Al_2O_3 (Cl) aged	2, 6	6, 3	44	
6U) Pt/meso Al_2O_3 (Acac)	23	58	4.9	
7U) Pt/nonporous Al_2O_3	weak	weak		16–24
8U) Pt/meso SiO_2 (3 nm)	19	46	6.0	4–20
9U) Pt/meso SiO_2 (3 nm) EXC	26	64	4.4	10–20
10U) Pt/meso SiO_2 (6 nm)	24	59	4.7	
11U) Pt/micro P SiO_2	66	162	1.7	
12U) Pt/micro J SiO_2	45	110	2.5	
13U) Pt/nonporous SiO_2	26	65	4.4	

Note. Metallic dispersion, metallic surface area, and particle diameter determined by H_2 chemisorption, particle diameter deduced from electron microscopy.

platinum precursor is not discernable, though, for a given support, i.e., the mesoporous alumina, the solids prepared with a chlorine-containing precursor (4U and 5U) both exhibit low dispersion (6.2 and 2.6%) and thus high intrinsic activity, but higher activity than the solid 3U (dispersion 12%) prepared with a chlorine-free precursor.

No relationship has been found between the N_2O selectivity, $N_2O/(N_2 + N_2O)$, which varies between 53 and 80% at the NO reduction maximum, and the initial or final dispersion.

In the literature, a comparable influence of the initial dispersion of Pt on the reactions occurring during SCR of NO by C_3 hydrocarbons has already been observed, especially with a silica support, for which the turnover frequency (TOF) of large particles (4% dispersion) is twice that of smaller ones (40% dispersion); with alumina, the effect is less significant (2,5,12). In another study, however, the TOF of NO oxidation into NO_2 becomes 100 times greater when the dispersion decreases from 82 to 4% on an alumina support, but the activity increase is less pronounced for NO reduction and much less pronounced for C_3H_6 oxidation (15). Furthermore, for a given reaction, such as NO oxidation into NO_2 or SO_2 oxidation into SO_3, the size dependency is significant with silica, less significant with alumina, and nonexistent with zirconia (17). Greater activity with larger particles has also been observed for NO dissociation (18,19), reduction of NO by CO or H_2 (18,19), and reduction of NO by CH_4 (16). Results concerning N_2O selectivity are contradictory: either the metal dispersion does not affect the N_2O selectivity (16), or more N_2O is produced over a more highly dispersed solid (15). In a study involving Pd, N_2O is not formed on small particles (20).

In the above studies, chemisorption measurements are performed only on fresh catalysts. Recently, however, Burch *et al.* considered the Pt dispersion after reaction and demonstrated that its weak value was due to low-temperature poisoning of Pt by carbonaceous deposits, despite the considerable O_2 excess of their NO–*n*-C_8H_{18}–O_2 reaction mixture (41). In our case (C_3H_6 as reductant), such low-temperature encroachment is improbable, since during the first of successive temperature increase–decrease cycles, the catalyst is activated (due to sintering), and no deactivation (or further activation) occurs for subsequent cycles. Additionally, the Pt particle size deduced from H_2 chemisorption is either equal to or smaller than that observed with TEM (Table 3); this would not occur if carbonaceous species had encapsulated the Pt.

CONCLUSION

During selective NO_x reduction under lean-burn conditions up to 773 K, the platinum particles sinter. The intrinsic activity increases with decreasing dispersion, regardless of whether the metallic surface area is measured before or after reaction, whatever the reaction: reductions of NO into N_2 and N_2O, oxidation of NO into NO_2, or oxidation of C_3H_6 into CO_2. An optimum in intrinsic activity was generally not observed, even with a dispersion as low as 2.6%. The Pt dispersion is a major factor affecting the intrinsic activity of the reactions, while the nature of the support (alumina or silica), the porosity and impurities of the support, and the nature of the platinum precursor are less important and not easily discernable. It seems that a solid prepared with a chlorine-containing precursor exhibits a higher activity than a solid prepared with a chlorine-free precursor.

An analogous particle size dependency, that takes into account the particle size before reaction, has been observed in the past for a variety of supports (2,5,12,15–20). This paper, however, highlights the changes in dispersion and particle size distribution that occur under the reactant mixture, since the initial state of the solids is not representative of the state after activation. Also, in contrast with other studies, a large range of initial metal dispersion has been considered. We have also taken various other parameters into account. Studies are under way to determine if the size dependency is linked to another factor, such as redox properties or strength of the Pt–NO bond.

ACKNOWLEDGMENTS

We thank Anne Julbe (Laboratoire des Matériaux et des Procédés Membranaires, Montpellier) and Catherine Pinel (Institut de Recherches sur la Catalyse, Villeurbanne) for the preparation of the microporous silica supports.

REFERENCES

1. Amiridis, M. D., Zhang, T., and Farrauto, R. J., *Appl. Catal. B* **10**, 203 (1996).
2. Burch, R., and Millington, P. J., *Catal. Today* **26**, 185 (1995).
3. Sasaki, M., Hamada, H., Kintaichi, Y., Ito, Y., and Tabata, M., *Catal. Lett.* **15**, 297 (1992).
4. Hirabayashi, H., Yahuro, H., Mizuno, N., and Iwamoto, M., *Chem. Lett.* 2235 (1992).
5. Burch, R., Millington, P. H., and Walker, A. P., *Appl. Catal. B* **4**, 65 (1994).
6. Amiridis, M. D., Roberts, K. L., and Pereira, C. J., *Appl. Catal. B* **14**, 203 (1997).
7. Iwamoto, M., Yahiro, H., Shin, H. K., Watanabe, M., Guo, J., Konno, M., Chikahisa, T., and Murayama, T., *Appl. Catal. B* **5**, L1 (1994).
8. Iwamoto, M., and Hamada, H., *Catal. Today* **10**, 57 (1991).
9. Hamada, H., Kintaichi, Y., Sasaki, M., Ito, T., and Tabata, M., *Appl. Catal.* **75**, L1 (1991).
10. Inaba, M., Kintaichi, Y., and Hamada, H., *Catal. Lett.* **36**, 223 (1996).
11. Burch, R., *Catal. Today* **35**, 27 (1997).
12. Burch, R., and Millington, P. J., *Catal. Today* **29**, 37 (1996).
13. Zhang, G., Yamaguchi, Y., Kawakami, H., and Suzuki, T., *Appl. Catal. B* **1**, L15 (1992).
14. Hamada, H., *Catal. Today* **22**, 21 (1994). [see references therein.]
15. Lee, J. H., and Kung, H. H., *Catal. Lett.* **51**, 1 (1998).
16. Demicheli, M. C., Hoang, L. C., Ménézo, J. C., Barbier, J., and Pinabiau-Carlier, M., *Appl. Catal. A* **97**, L11 (1993).
17. Xue, E., Seshan, K., and Ross, J. R. H., *Appl. Catal. B* **11**, 65 (1996).
18. Otto, K., and Yao, H. C., *J. Catal.* **66**, 229 (1980).

19. Kaspar, J., de Leitenburg, C., Fornasiero, P., Trovarelli, A., and Graziani, M., *J. Catal.* **146**, 136 (1994).
20. Xu, X., and Goodman, D. W., *Catal. Lett.* **24**, 31 (1994).
21. Sato, S., Yu-u, Y., Hahiro, H., Mizuno, N., and Iwamoto, M., *Appl. Catal.* **70**, L1 (1991).
22. Shelef, M., *Chem. Rev.* **95**, 209 (1995).
23. Perrichon, V., *J. Soc. Alg. Chim.* **3S**(1), 1 (1993). [see references therein.]
24. Julbe, A., Balzer, C., Barthez, J. M., Guizard, C., Larbot, A., and Cot, L., *J. Sol-Gel Sci.Technol.* **4**, 89 (1995).
25. Chajar, Z., Primet, M., Praliaud, H., Chevrier, M., Gauthier, C., and Mathis, F., *in* "Studies in Surface Science and Catalysis" (A. Frennet and J. M. Bastin, Eds.), Vol. 96, p. 591. Elsevier, Amsterdam, 1995.
26. Chajar, Z., Primet, M., Praliaud, H., Chevrier, M., Gauthier, C., and Mathis, F., *Appl. Catal. B* **4**, 199 (1994).
27. Chajar, Z., Primet, M., Praliaud, H., Chevrier, M., Gauthier, C., and Mathis, F., *Catal. Lett.* **28**, 33 (1994).
28. Li, Y., and Hall, W. K., *J. Phys. Chem.* **94**, 6145 (1990).
29. Keefer, K. D., Schaefer, D. W., and Ashley, C. S., *J. Non-Cryst. Solids* **48**, 47 (1982).
30. Briot, P., Auroux, A., Jones, D., and Primet, M., *Appl. Catal.* **59**, 141 (1990).
31. Briot, P., and Primet, M., *Appl. Catal.* **68**, 301 (1991).
32. Baldwin, T. R., and Burch, R., *Appl. Catal.* **66**, 337 and 359 (1990).
33. Hoyos, L. J., Praliaud, H., and Primet, M., *Appl. Catal. A* **98**, 125 (1993).
34. Obuchi, A., Ohi, A., Nakamura, M., Ogata, A., Mizuno, K., and Obuchi, H., *Appl. Catal. B* **2**, 71 (1993).
35. Captain, D. K., Roberts, R. L., and Amiridis, M. D., *Catal. Today* **42**, 93 (1998).
36. Burch, R., and Watling, T. C., *Appl. Catal. B* **11**, 207 (1997).
37. Li, Y., and Armor, J. N., *Appl. Catal. B* **1**, L21 (1992).
38. Carballo, L. M., and Wolf, E. E., *J. Catal.* **53**, 366 (1978).
39. Hicks, R. F., Qi, H., Young, M. L., and Lee, R. G., *J. Catal.* **122**, 280 and 295 (1990).
40. Duplan, J. L., and Praliaud, H., *in* "Studies in Surface Science and Catalysis" (A. Crucq, Ed.), Vol. 71, p. 667. Elsevier, Amsterdam, 1991.
41. Burch, R., Fornasiero, P., and Southward, B. W. L., *J. Catal.* **182**, 234 (1999).